Journal of Physics:
Conference Series

PAPER • **OPEN ACCESS**

Experimental campaign on the chemical composition of aluminium powders for hydrogen production

To cite this article: Silvia Barbi *et al* 2025 *J. Phys.: Conf. Ser.* **3143** 012017

Journal of Physics: Conference Series **3143** (2025) 012017 doi:10.1088/1742-6596/3143/1/012017

Experimental campaign on the chemical composition of aluminium powders for hydrogen production

Silvia Barbi[1], Matteo Venturelli*[1], Alessandro Montagneretto Olivari[1], Monia Montorsi[1], Nicola Musicco[2], Marcello Gelfi[2], Massimo Milani[1], Luca Montorsi[1]

[1] Department of Sciences and Methods for Engineering, University of Modena and Reggio Emilia, Italy
[2] Department of Mechanical and Industrial engineering, University of Brescia, Brescia, Italy

*E-mail: matteo.venturelli@unimore.it

Abstract. The reaction between aluminium and water has garnered significant interest in materials science due to its promising applications, particularly in hydrogen production. In this context, repurposing aluminium powder derived from waste presents a potentially sustainable pathway for low-impact hydrogen generation. This study explores the reaction mechanisms of various waste-sourced aluminium powders under different heating procedures in an uncontrolled (air) atmosphere. Post-reaction, the samples were analyzed using scanning electron microscopy (SEM) to assess their morphology, alongside energy-dispersive spectroscopy (EDS) for semi-quantitative chemical composition. Additionally, Rietveld refinement was applied to X-ray diffraction (XRD) data to identify the resulting crystalline compounds. The analysis revealed the formation of several aluminium-based compounds (such as AlN, Al_2O_3, Al_2MgO_4), with no trace of pure aluminium remaining after thermal treatment. This finding highlights the high reactivity of the tested waste powders. Overall, the study offers valuable insights into the reaction pathways of aluminium powders and supports the potential of using waste aluminium in hydrogen production processes.

1. Introduction

In recent years, the escalating global pollution levels and the proliferation of particulate matter have raised significant concerns within the international scientific community. Consequently, there has been a concerted effort to explore environmentally sustainable pathways towards a cleaner energy economy [1].

Within this framework, two viable solutions for mitigating environmental emissions involve the enhancement of energy efficiency in existing systems and the exploration of alternative energy vectors to replace fossil fuels. Among these alternatives, hydrogen emerges as a particularly promising energy vector, as evidenced by various studies. For instance, Yilmaz et al.[2] have

investigated the use of hydrogen for achieving fuel independence, while another study [3] delves into its application in domestic settings, focusing on the innovative design of burners for stoves. Furthermore, the application of hydrogen technology extends to the transportation sector, where it powers vehicles, offering a zero-emission mode of transportation [4][5]. However, despite its promise, clean hydrogen production with minimal environmental impact remains a major obstacle, as highlighted in recent research [6][7].

Traditionally, hydrogen is primarily produced through processes that rely on fossil sources, contributing to greenhouse gas emissions [8] [9]. For example, natural gas steam reforming generates approximately 7.5 kg of carbon dioxide per kilogram of hydrogen [8]. Alternatively, Holladay et al. [9] have reviewed hydrogen production processes with lower environmental footprints, such as water electrolysis and hydrogen production from biomass or nuclear energy. Nonetheless, the challenges associated with the low density of hydrogen make its transportation and storage costly [10]. Consequently, addressing the costs related to hydrogen delivery and storage is imperative for its wider adoption in an eco-friendly energy economy.

Sustainable on-site hydrogen production may be realized by chemical reduction of H2 from water, as for this procedure not distilled water is suitable and an external power source is not required, but only a reductant compound. The hydrogen production in even more sustainable way is an issue that is gaining more and more attention to increase the production efficiency by lowering its environmental impact at the same time.

In the realm of literature, an innovative methodology that addresses existing challenges can be found in the interaction of metals with water, particularly in the production of hydrogen with zero carbon emissions. This approach centers around the concept of utilizing metals as energy carriers. A notable example is the exploration of aluminum's reaction with water due to its high hydrogen production rate and substantial energy release [11]. This intriguing reaction has garnered attention in diverse applications, including marine [12] and aerospace [13] contexts.

In the existing body of literature, a majority of studies on aluminum combustion predominantly focus on the reaction of aluminum particles with water to yield hydrogen. Swamy and Shafirovich, in [14], delved into the viability of converting aluminum scrap, including foil, into activated aluminum powders that chemically split water, releasing hydrogen. Vlaskin explored a cogeneration plant utilizing the reaction between metallic powder and water at 330°C [15].

One of the main disadvantages of using aluminum powders is the formation of a compact oxidation layer of Aluminium Oxide on the surfaces' particles which hinder further hydrolysis reaction and reduces the hydrogen production yield. Thereafter an increasing number of recent works have been devoted to a detailed analysis of the aluminium and Al-based compounds suitable for electrolysis. In particular, a possible pathway under investigation is the doping of Aluminium with other elements such as Ga, In, Sn, Mg, Cu, Zn, Li, Bi, Fe or oxides, hydrides, nitrides and chlorides to activate Aluminium reactivity with water. The proposed mechanism is that activators and Aluminium could generate micro galvanic cells and/or porosities capable to open the way to water to the Aluminium non-oxidized surface and across the thick oxide film

Mercati et al. [16] provided a detailed analysis and description of a system that integrates hydrogen production with thermal and electrical power generation by utilizing liquid aluminium injection. Limited data on the reaction of liquid aluminum with water is available, with notable contributions from Milani et al. [17] [18]. The environmental profile of the system was examined in [19], revealing that the primary contributor to the overall environmental impact is the production of liquid aluminium, mainly due to the use of natural gas.

In this context, the present work aims to investigate the reactivity of different aluminium-based powders, by-products from aluminum casting process, to assess whose hydrolysis process can be easily controlled to produce hydrogen stably.

This work presents a novel experimental approach to valorize aluminum waste powders for sustainable hydrogen production through water-based reactions. Unlike conventional studies that rely on high-purity aluminum or complex activation methods, this analysis focuses on by-products from industrial processes—materials typically considered waste. By applying controlled thermal treatments and coupling detailed morphological, chemical, and crystallographic analyses, the study reveals the inherent reactivity of these powder, a crucial step toward understanding and optimizing their behavior in aluminium-water reactions.

Following the experimentation, the samples underwent analysis using scanning electron microscopy to ascertain their morphology. Additionally, energy dispersive spectroscopy was employed to assess their semi-quantitative chemical composition. Moreover, X-ray diffraction spectra underwent Rietveld refinement to estimate the formulation of reaction products in terms of crystalline compounds.

2. Materials and Methods

2.1 Materials

Two powders (POWDER 1 and POWDER 2) have been considered in this study, as outcome of a casting process. The powders are the scraps of the aluminum casting process and they represents a cost for companies since they are forced to dispose these wastes to landfill. The detailed characterization of both powders has been reported in the Results section but, it must be underlined that a Calcium-based pollutant content is expected to be the principal difference in their formulation that could drive the formation of different compounds after the heating cycle.

Heating treatments

Heating treatments have been carried out in a laboratory furnace (CWF 12/65 – Carbolite GERO) having air as atmosphere and chamber volume of 65 l. Powders have been collocated in porcelain crucibles, having maximum volume equal to 100 ml. Two different heating treatments have been applied to both the powders, having different temperature steps as reported in Figure 1. For both the heating cycles, the highest temperature reached has been 1200 °C at a heating rate of 5 °C/min, according to the limits of the furnace in terms of the highest temperature and slowest heating rate achievable. The lowest temperature, related to the heating cycle 1, has been selected as near to the theoretical Aluminium melting point (660 °C). To simplify the reader comprehension in Table 1 the samples labelling has been summarized.

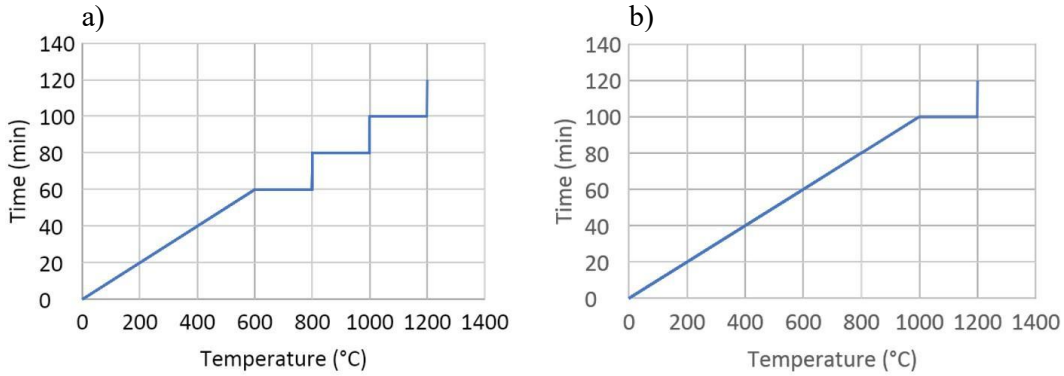

Figure 1. Heating treatments employed in this study a) Heat Treatment 1 b) Heat Treatment 2

Table 1. Investigated samples.

.

LAbel	Sample description
POWDER 1	Powder 1 as it is
POWDER 2	Powder 2 as it is
P1_HT1	Sample obtained after heat treatment 1 applied to POWDER 1

Characterizations

Weight measurements were carried out using an analytical balance with a sensitivity of 0.0001 g and a maximum capacity of 100 g. The particle size and morphology of the as-received powders were examined using environmental scanning electron microscopy (ESEM, FEI XL-30), coupled with energy-dispersive spectroscopy (EDS) to obtain semi-quantitative chemical compositions. The EDS spectra presented in this study represent averages derived from at least five different regions of each sample.

The crystalline phases present in the samples before and after each heat treatment were identified via X-ray Powder Diffraction (XRPD, X'Pert PRO, PANalytical). Data acquisition was performed using a θ/θ diffractometer with Cu Kα radiation and a Real Time Multiple Strip (RTMS) detector. The diffractometer was equipped with 0.5° divergence and anti-scattering slits, along with a 0.04 rad Soller slit on the incident beam path. A Ni filter and a 5 mm anti-scatter blade were placed on the diffracted beam path. A virtual step scan was conducted with a step size of 0.0167° 2θ and a counting time of 50 seconds per step, ensuring high counting statistics.

To minimize preferred orientation effects, powder samples—typically composed of randomly oriented crystallites—were prepared using side-loading in aluminium sample holders [20].

Rietveld refinements were performed using the PANalytical X'Pert PRO software package. Standardization was achieved by analyzing the XRPD pattern of α-quartz (NIST SRM 1878b), using the same instrumental configuration as for the test samples. Literature values for certified lattice parameters were used to fix structural parameters and calibrate the Kα1/Kα2 ratio, polarization, and profile shape parameters (GW, LX, LY, and Asym) within the "type 2" profile model. This standardized approach to refinement is essential due to the significant correlations among scale factors, profile parameters, and preferred orientation corrections, particularly for clay phases with substantial peak overlap [21].

3. Results and discussion

3.1 Raw powders

Powders morphology has been investigated through ESEM at different magnification and results are represented in Figure 2, together with the average spectra obtained by the semi quantitative chemical analysis conducted with EDS. Morphological analysis is carried out with secondary electrons (ETD). As shown in Figure 2a and Figure 2b at low magnification (250X), there are no particular differences between the powders, as both powders are found to be homogeneous and without any particular agglomerates. At high magnification (1000X), a rather similar morphology is confirmed between the two specimens with particles having a size of approximately 10 micrometers (according to the scale bar). However, in POWDER 2, few larger agglomerates (up to 50 micrometers of diameter) can be measured. The semi quantitative chemical analysis achievable by EDS (Figure 2e and Figure 2f) indicate that in POWDER 1 only Aluminum and Oxygen are present, whereas in POWDER 2 also the presence of Calcium and Magnesium in addition to Aluminum and Oxygen can be observed. Moreover, it should be noted that the clusters present in the morphological analysis of POWDER 2 were analyzed trough EDS but without finding a particular different chemical formulation from the overall sample.

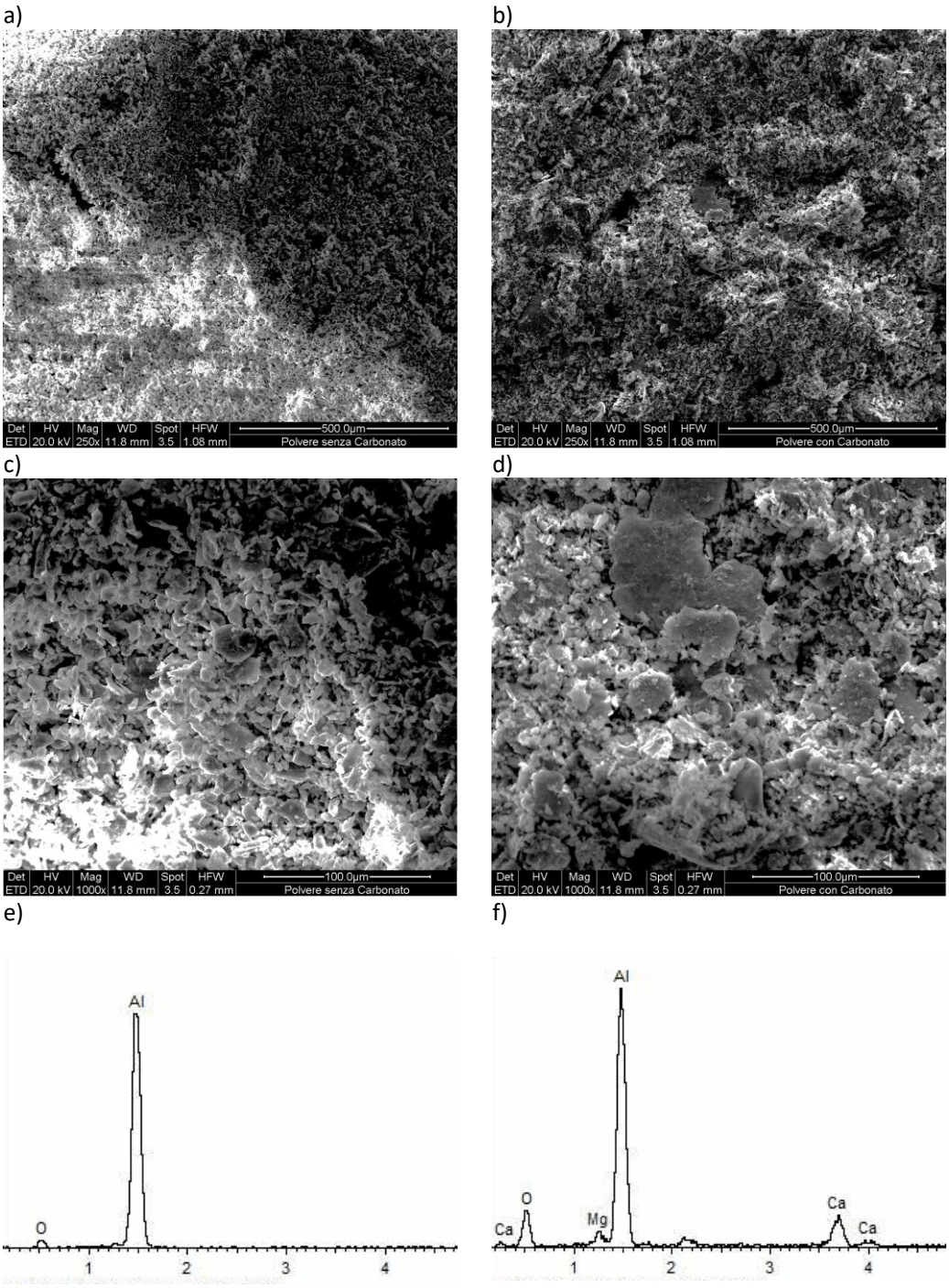

Figure 2. ESEM micrograph of raw powders: a) POWDER 1 at 250X; b) POWDER 2 at 250X; c) POWDER 1 at 1000X; d) POWDER 2 at 1000X; e) POWDER 1 EDS spectra; f) POWDER 2 EDS spectra.

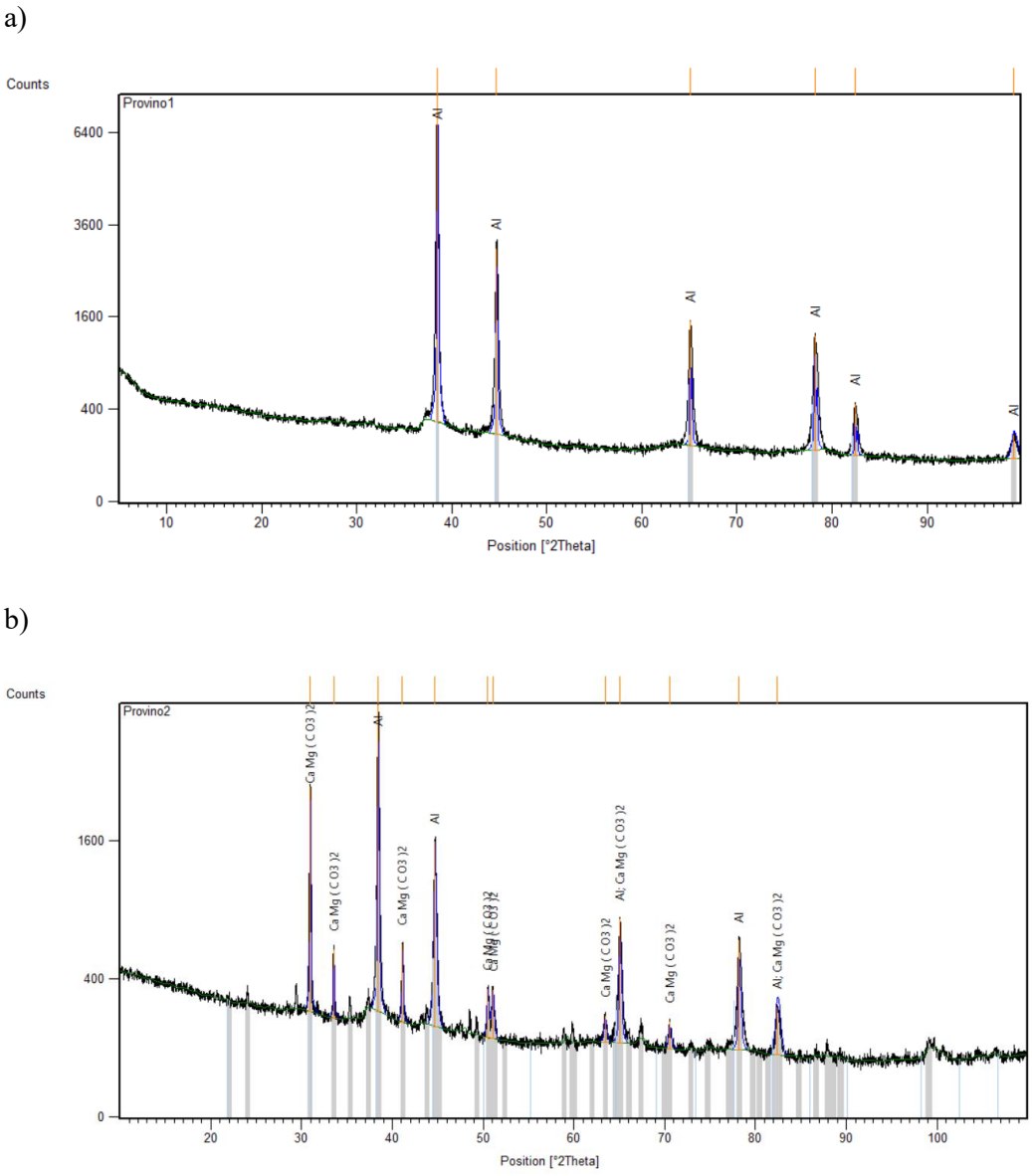

Figure 3. XRD Spectra of the raw powders: a) POWDER 1; b) POWDER 2

From the XRD spectra reported Figure 3a is clear that the only crystalline phase present in POWDER 1 is Aluminum (Al - ICDD: 03-065-2869). No bands corresponding to the presence of amorphous material are evident, so all of the sample can be addressed to be 100% metallic Aluminum and for this reason this specimen will not be subject to quantitative Rietveld analysis. In POWDER 2 (Figure 3b), unlike Specimen 1, two crystalline phases coexist: metallic Aluminum (Al - ICDD: 03-065-2869) and Dolomite, or Calcium Magnesium Carbonate (CaMgC2O6 - ICDD: 00-036-0426). Therefore, quantitative Rietveld analysis was needed to estimate the amount of either phase. The results of the Rietveld analysis estimated a CaMgC2O6 content of about 4 %, with the remaining 96 % being metallic Aluminum. The order of magnitude of absolute errors on

the Rietveld analysis is 1 %. Coherently with POWDER 1, no bands corresponding to the presence of amorphous material can be detected, indicating that also this sample is totally crystalline.

3.2 Powder after the heat treatment

In Figure 4 and in Table 2 are reported two physical observations of the samples obtained after the complete heat treatment. In Figure 4 colour changing during the heat treatment and among POWDER 1 and POWDER 2 indicate that different reactions occur in the samples, in particular for POWDER 2 it can be observed a clear phase separation of white colour on the surface of the sample during and after both Heat treatment 1 and 2. On the opposite POWDER 1 show a totally white sample during each heating treatment, indicating probably an increasing volume of alumina, that have a white colour.

Regarding weight observation the precise starting weight for each different sample has been reported in Table 2, as well as weight variation during heating treatment. Also in this case, differences among samples can be detected as during the POWDER 2 treatment a decreasing in weight is observed, probably due to the carbonate reaction with the increasing temperature. On the opposite POWDER 1 treatment results in an increased weight with the increasing temperature, suggesting a changing in sample structure, probably, from metallic Aluminum (density = 2.7g/cm3) to Alumina (density = 3.95 g/cm3). Nevertheless, comparing density variation (+ 46 %) with weight variation after the first heating treatment (+39 %) it can be concluded that other crystalline phases than Alumina only should be present in sample P1_HT1. And the same is for sample P1_HT2, considering a weight variation equal to + 36%.

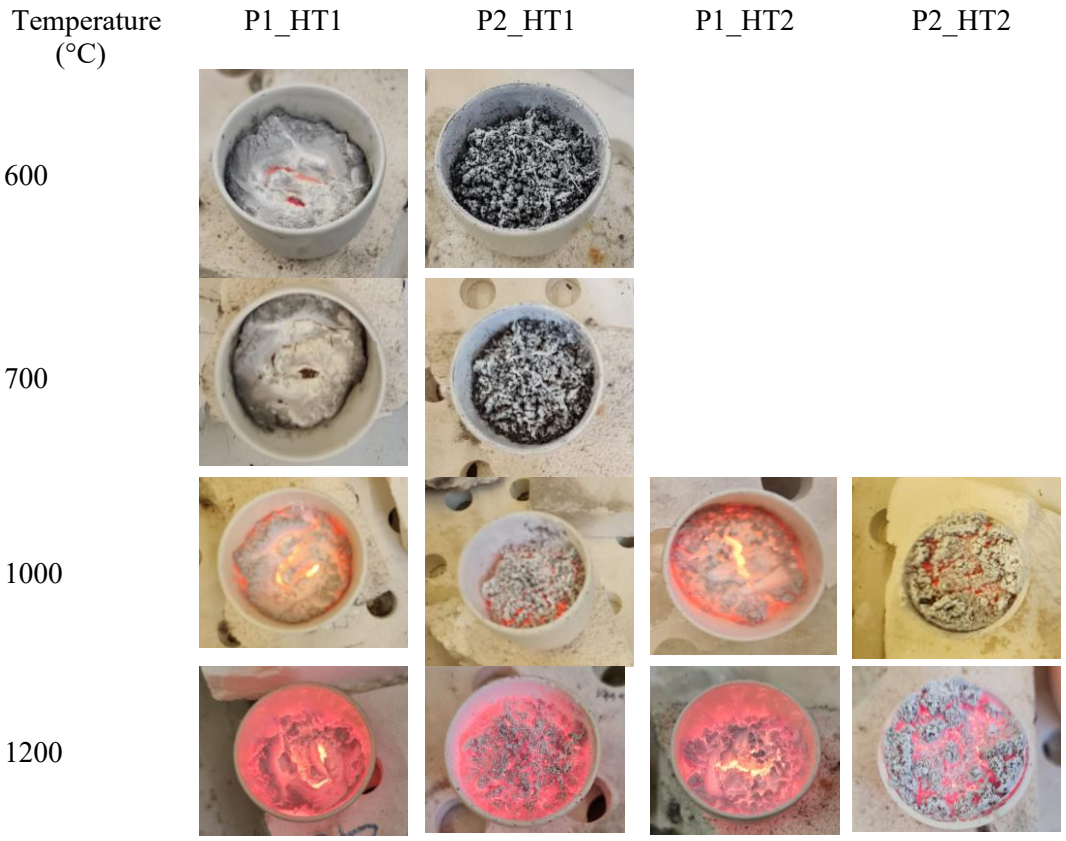

Figure 4. Samples appearance during the heat treatments

Table 2. Weight (g) of samples measured before and after the heating treatments.

Temperature (°C)	P1_HT1	P2_HT1	P1_HT2	P2_HT2
25	10.7144	11.0075	10.6486	10.1204
600	13.5565	10.0739	/	/
800	13.5587	10.0669	/	/
1000	14.0845	10.4527	13.8354	8.5320
1200	14.8686	10.7471	14.4952	8.7611

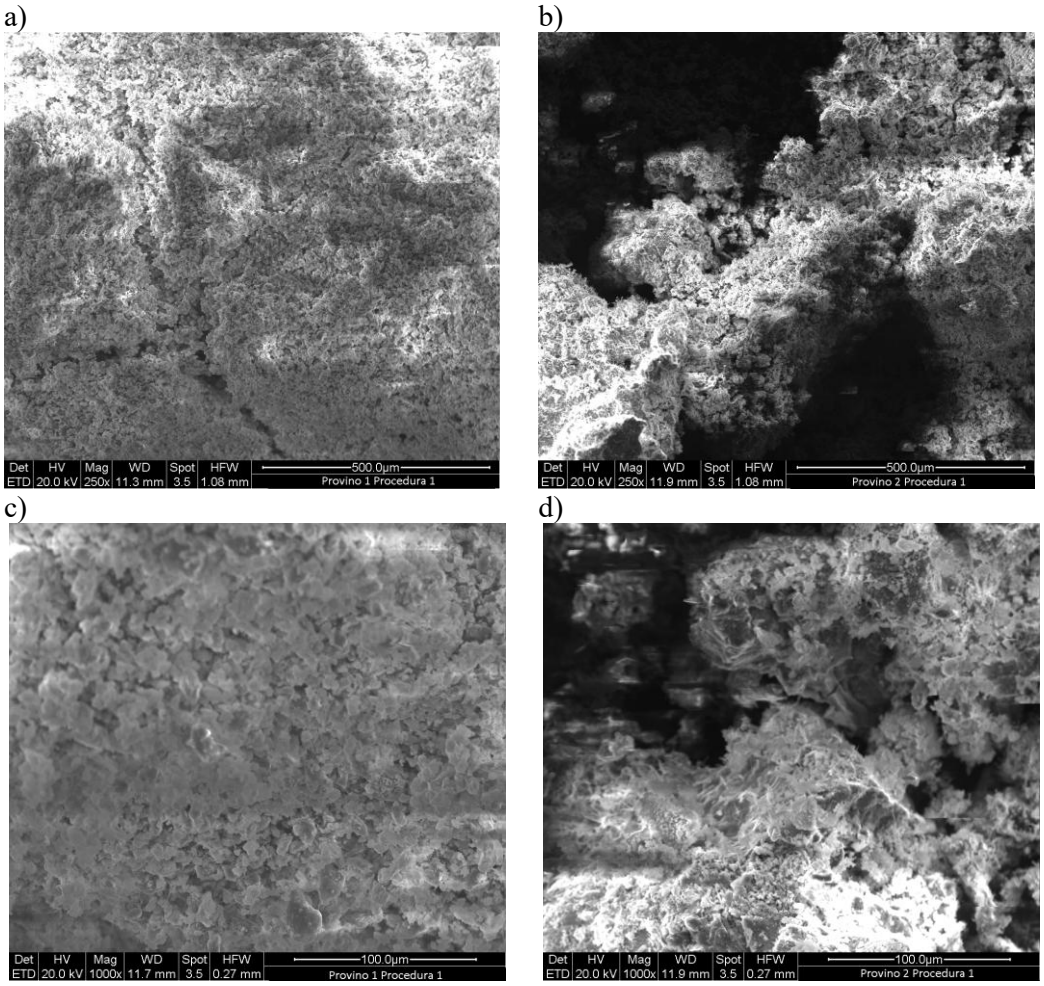

Figure 5. ESEM micrograph of samples after the heat treatment 1: a) P1_HT1 at 250X; b) P2_HT1 at 250X; c) P1_HT1 at 1000X; d) P2_HT1 at 1000X

The morphology of the samples obtained after the first heat treatment are reported in Figure 5. POWDER 1 (Figure 5a and 5c) shows a porous but homogeneous microstructure with only the presence of macrocracks visible at 250X most likely due to the rapid cooling of the sample. The porosity of the P1_HT1 is mostly closed. In contrast P2 _HT1 (Figure 5b and 5d) shown a strongly porous microstructure with open and inhomogeneous pore, as they are heterogeneously spread into the microstructure and having highly variable dimensions.

Indeed, after the second heat treatment (Figure 6) both powders results in a very porous microstructure, with open porosity and formation of one or more crystalline phases having a "filamentous" shape, suggesting the formation of different crystalline phases with respect to heat treatment 1. Even if with limitation, also in this case a little bit more compact structure is observed for the sample obtained from POWDER 1, thereafter P1_HT2, in fact, a reduced porosity and a rather heterogeneous microstructure is to be noted for this sample.

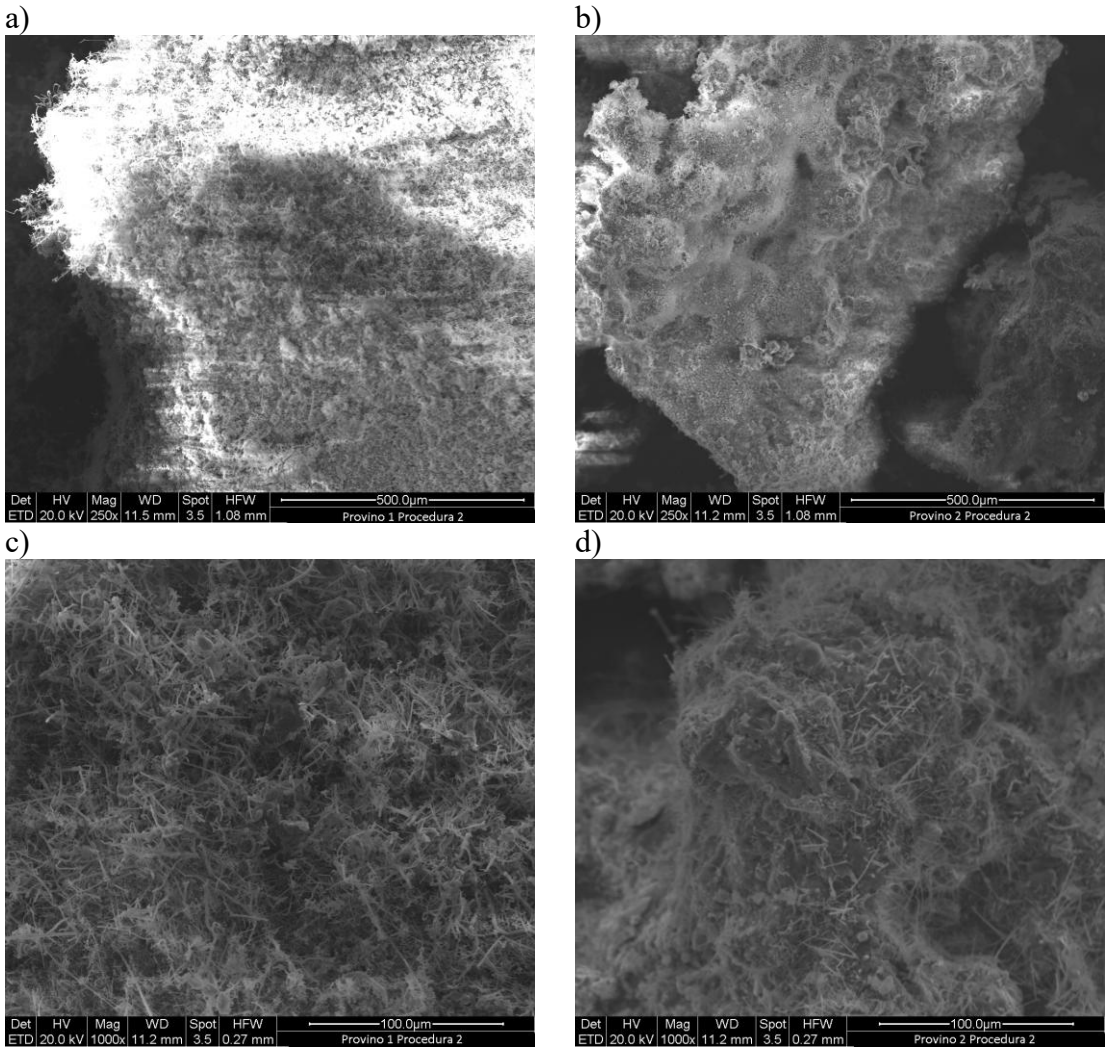

Figure 6. ESEM micrograph of samples after the heat treatment 2: a) P1_HT2 at 250X;b) P2_HT2 at 250X; c) P1_HT2 at 1000X; d) P2_HT2 at 1000X

a)

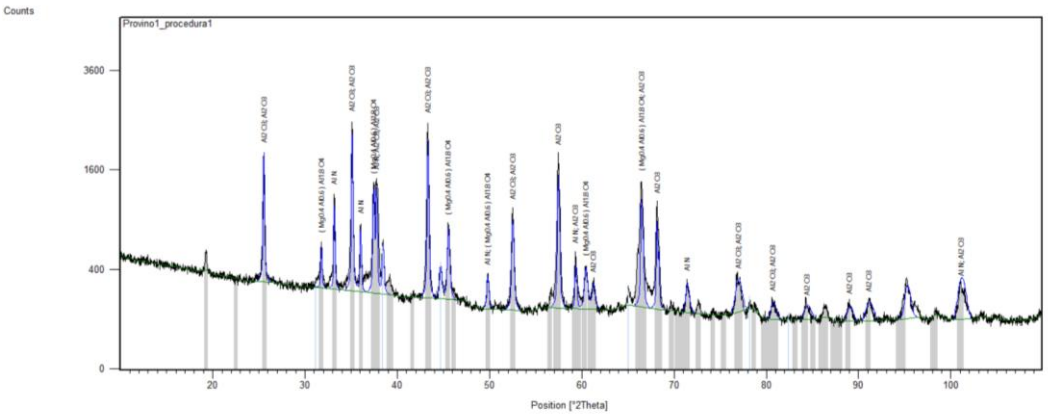
Counts
Provino1_procedura1
Position [°2Theta]

b)

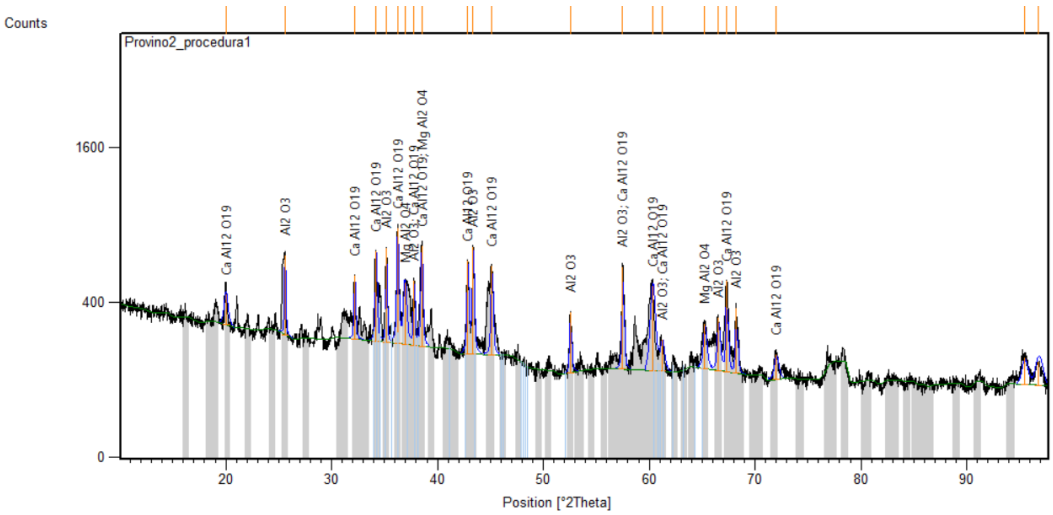
Counts
Provino2_procedura1
Ca Al12 O19
Al2 O3
Mg Al2 O4
Position [°2Theta]

c)

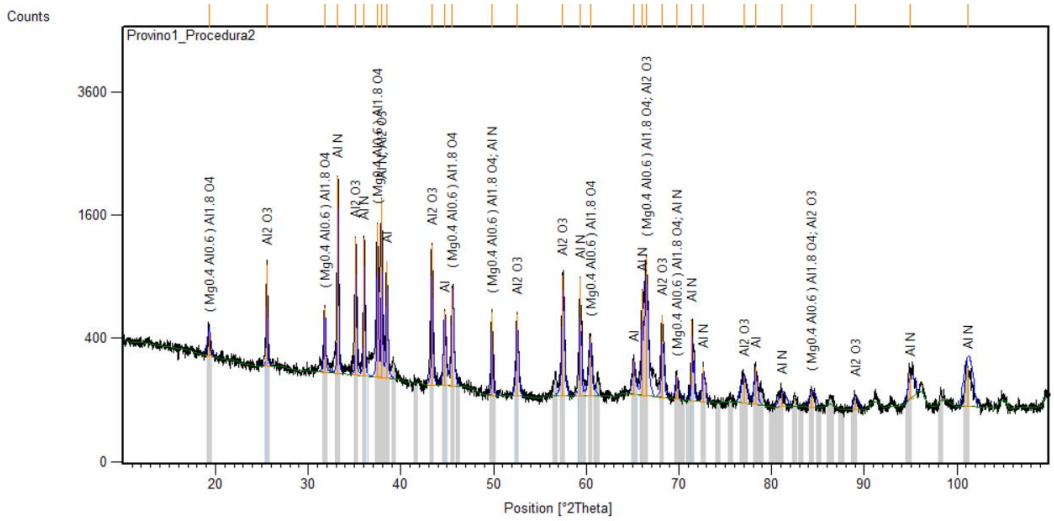
Counts
Provino1_Procedura2
(Mg0.4 Al0.6) Al1.8 O4
Al2 O3
Al N
Al
Position [°2Theta]

d)

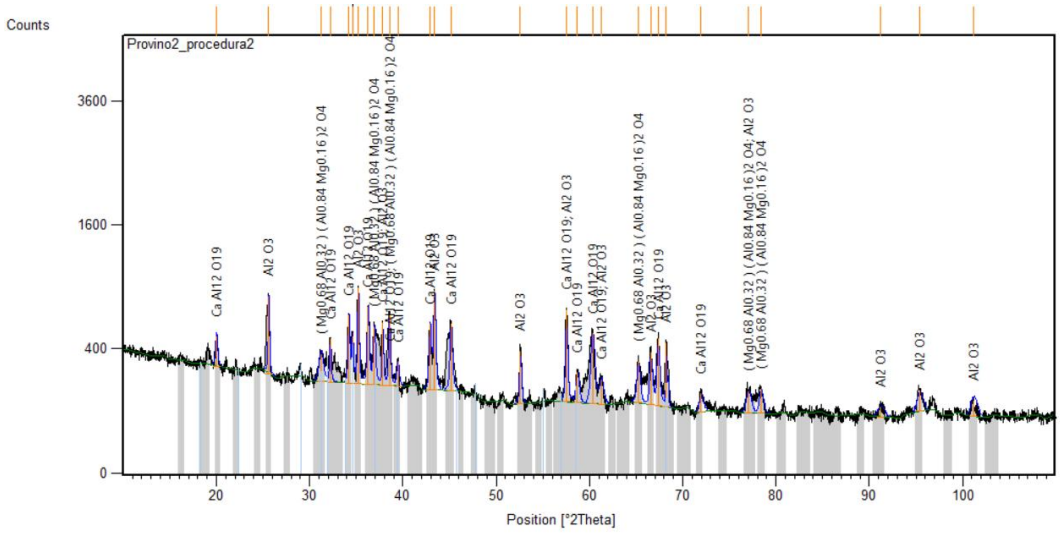

Figure 7. XRD spectra of samples after the heat treatments: a) P1_HT1; b) P2_HT2 ; c) P1_HT2; d) P2_HT2

To further investigate crystalline phases formation after the heating treatments XRD spectra have been collected and Rietveld refinement have been conducted. All the sample are characterized by several crystalline phases and no band attributable to amorphous phase is present. Notably, all the metallic aluminum present is capable to converts to aluminum compounds with only one exclusion that is P1_HT2. Rietveld refinement results have been summarized in Figure 8 for better comprehension.

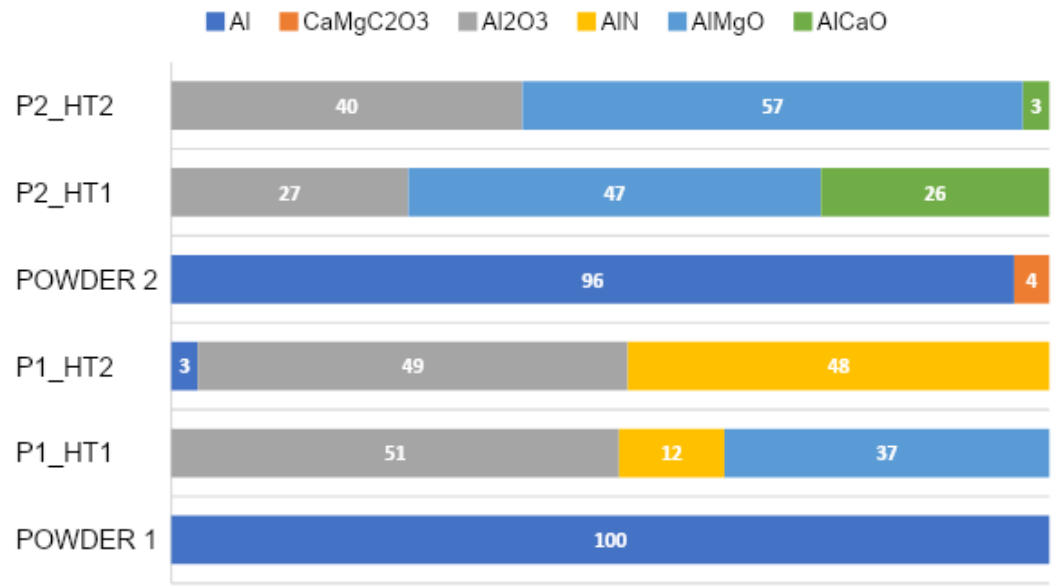

Figure 8. Summary of the crystalline phases identified after the Rietveld refinement (Absolute error 1%). Al - ICDD: 01-089-2769 ; Al2O3 - ICDD: 01-075-1865; AlN - ICDD: 00-008-0262 ; AlMgO - ICDD: 01-087-0345 ; AlCaO - ICDD: 00-025-0122 ;

3.3. Discussion

Regarding the two analyzed powders, as expected, a difference in the chemical and microstructural formulation has been assessed. In particular in POWDER 2 Calcium and Magnesium are present in the form of their binary carbonate (4%) . It can be noted that, in this case, the XRD analysis is completely consistent with the ESEM-EDS, nevertheless, semi-quantitative chemical analysis has some limitations: (i) very low sampling volume (ii) relatively high errors on the measurements, especially in the case of the presence of many elements and/or light elements, (iii) difficulty in identifying elements in low amount as the detection limit is 0.5 %. In addition, the microstructure of POWDER 2 is characterized by clusters not assignable to specific crystalline phases. Taking in account these differences, the employment of these two powders in the heating treatment can be useful for comparison of different possible reactivity of Aluminum based powders.

Taking in account the samples after the heat treatment, it results clear that the presence of carbonates in POWDER 2 results in samples with an opener porosity after the heating treatment, leading to a less compact structure and thereafter suggesting an easier penetration of water and promoted reactivity with respect to Aluminum. In this sense the first heat treatment (P2_HT1) should be preferred as a lower amount of Alumina is formed. Regarding the results obtained from POWDER 1 it is notable that the second heat treatment is not capable to transform all the metallic Aluminum, as a residue of 2 % has been detected.

4. Conclusion

In this comprehensive study, the intricate reaction mechanisms exhibited by various aluminum powders derived from waste sources when subjected to diverse heating procedures in an uncontrolled atmosphere, specifically in air, has been analysed and investigated. The investigative approach involved a meticulous analysis of the samples through scanning electron microscopy coupled with energy dispersive spectroscopy, unraveling their morphological characteristics and semi-quantitatively assess the chemical composition of the samples.

Furthermore, a Rietveld refinement to the X-ray diffraction spectra has been conducted, aiming to elucidate the formulation of reaction products in terms of crystalline compounds.

The outcomes of the experiments unequivocally revealed the intricate chemical transformations that aluminum powders engaged with the ambient air, resulting in the formation of distinct aluminum compounds such as AlN, Al2O3, Al2MgO4, among others. Notably, a significant revelation emerged from our study— the conspicuous absence of pure aluminum following the thermal treatment. This absence underscores the remarkably reactive nature of the investigated waste powders during the heating process.

In essence, the study not only sheds light on the reaction mechanisms of aluminum powder but also highlights a pivotal observation: the robust reactivity of waste aluminum powders, which, crucially, precludes the retention of pure aluminum. This insight holds immense promise for the utilization of waste aluminum as a resource in the generation of hydrogen, thereby offering a valuable contribution to the sustainable and innovative exploitation of aluminum waste streams.

5. References

[1] M. Venturelli, E. Falletta, C. Pirola, F. Ferrari, M. Milani, and L. Montorsi, "Experimental evaluation of the pyrolysis of plastic residues and waste tires," Appl. Energy, vol. 323, no. July, p. 119583, 2022, doi: 10.1016/j.apenergy.2022.119583.
[2] I. Yilmaz, M. Ilbaş, M. Taştan, and C. Tarhan, "Investigation of hydrogen usage in aviation industry," Energy Convers. Manag., vol. 63, pp. 63–69, 2012, doi: 10.1016/j.enconman.2011.12.032.
[3] C. Y. Wu, K. H. Chen, and S. Y. Yang, "Experimental study of porous metal burners for domestic stove applications," Energy Convers. Manag., vol. 77, no. x, pp. 380–388, 2014, doi: 10.1016/j.enconman.2013.10.002.
[4] V. Bisaria and R. J. B. Smith, "Hydrogen production by onboard gasoline processing - Process simulation and optimization," Energy Convers. Manag., vol. 76, pp. 746–752, 2013, doi: 10.1016/j.enconman.2013.08.006.
[5] S. Sharma and S. K. Ghoshal, "Hydrogen the future transportation fuel: From production to applications," Renew. Sustain. Energy Rev., vol. 43, pp. 1151–1158, 2015, doi: 10.1016/j.rser.2014.11.093.
[6] P. A. Pilavachi, A. I. Chatzipanagi, and A. I. Spyropoulou, "Evaluation of hydrogen production methods using the Analytic Hierarchy Process," Int. J. Hydrogen Energy, vol. 34, no. 13, pp. 5294–5303, 2009, doi: 10.1016/j.ijhydene.2009.04.026.
[7] B. M. Besancon, V. Hasanov, R. Imbault-Lastapis, R. Benesch, M. Barrio, and M. J. Mølnvik, "Hydrogen quality from decarbonized fossil fuels to fuel cells," Int. J. Hydrogen Energy, vol. 34, no. 5, pp. 2350–2360, 2009, doi: 10.1016/j.ijhydene.2008.12.071.
[8] R. Kothari, D. Buddhi, and R. L. Sawhney, "Comparison of environmental and economic aspects of various hydrogen production methods," Renew. Sustain. Energy Rev., vol. 12, no. 2, pp. 553–563, 2008, doi: 10.1016/j.rser.2006.07.012.
[9] J. D. Holladay, J. Hu, D. L. King, and Y. Wang, "An overview of hydrogen production technologies," vol. 139, pp. 244–260, 2009, doi: 10.1016/j.cattod.2008.08.039.
[10] J. O. Abe, A. P. I. Popoola, E. Ajenifuja, and O. M. Popoola, "Hydrogen energy, economy and storage: Review and recommendation," Int. J. Hydrogen Energy, vol. 44, no. 29, pp. 15072–15086, 2019, doi: 10.1016/j.ijhydene.2019.04.068.
[11] Y. Yavor, S. Goroshin, J. M. Bergthorson, D. L. Frost, R. Stowe, and S. Ringuette, "Enhanced hydrogen generation from aluminum-water reactions," Int. J. Hydrogen Energy, vol. 38, no. 35, pp. 14992–15002, 2013, doi: 10.1016/j.ijhydene.2013.09.070.
[12] G. Roy, "Chemical Propulsion," 2001, doi: 10.1201/9781420040685.ch30.
[13] US DOE, "Reaction of aluminum with water to produce hydrogen," US DOE Rep., pp. 1–26, 2008, [Online]. Available: http://scholar.google.com/scholar?hl=en&btnG=Search&q=intitle:Reaction+of+Aluminum+with+Water+to+Produce+Hydrogen#0.
[14] A. K. Narayana Swamy and E. Shafirovich, "Conversion of aluminum foil to powders that react and burn with water," Combust. Flame, vol. 161, no. 1, pp. 322–331, 2014, doi: 10.1016/j.combustflame.2013.08.017.
[15] M. S. Vlaskin et al., "An experimental aluminum-fueled power plant," J. Power Sources, vol. 196, no. 20, pp. 8828–8835, 2011, doi: 10.1016/j.jpowsour.2011.06.013.
[16] S. Mercati, M. Milani, L. Montorsi, and F. Paltrinieri, "Design of the steam generator in an energy conversion system based on the aluminum combustion with water," Appl. Energy, vol. 97, pp. 686–694, 2012, doi: 10.1016/j.apenergy.2012.01.028.
[17] M. Milani et al., "Experimental and Numerical Analysis of a Liquid Aluminium Injector for an Al-H2O based Hydrogen Production System," Int. J. Thermofluids, p. 100018, 2020, doi: 10.1016/j.ijft.2020.100018.
[18] M. Milani, L. Montorsi, G. Storchi, and M. Venturelli, "CFD analysis and experimental measurements of the liquid aluminum spray formation for an Al–H2O based hydrogen production system," Int. J. Hydrogen Energy, vol. 46, no. 59, pp. 30615–30624, 2021, doi: 10.1016/j.ijhydene.2021.01.119.
[19] M. Pini et al., "Life cycle assessment of an innovative cogeneration system based on the aluminum combustion with water," Renew. Energy, vol. 154, 2020, doi: 10.1016/j.renene.2020.03.046.
[20] A. F. Gualtieri, "Accuracy of XRPD QPA using the combined Rietveld-RIR method," J. Appl. Crystallogr., vol. 33, no. 2, pp. 267–278, 2000, doi: 10.1107/S002188989901643X.
[21] A. F. Gualtieri et al., "Quantitative phase analysis using the Rietveld method: Towards a procedure for checking the reliability and quality of the results," Period. di Mineral., vol. 88, no. 2, pp. 147–151, 2019, doi: 10.2451/2019PM870.